A Field-Portable Thermal Infrared Grating Spectrometer (THIRSPEC)

Benoit Rivard, Paul J. Thomas, D. Pollex, A. Hollinger, John R. Miller, and R. Dick

Abstract—**A thermal infrared grating spectrometer was developed for field studies in the earth sciences. The design is based on a reflection grating and a 60-element HgCdTe detector array. The useful spectral range of the instrument covers 7.9–11.3 μm with a Nyquist limited resolution of 0.16 μm. The instrument averages over a 12° field of view and compares the exitance of the target to that of an internal black body at ambient temperature. The noise equivalent temperature is approximately 0.06°K over the useful spectral range. Background radiance reflected from the surface of the target can seriously impede the determination of emissivity. This effect is removed from the spectra of geological samples by the use of reference samples.**

I. Introduction

THE Thermal InfraRed SPECtrometer (THIRSPEC) is a 60-channel array spectroradiometer operating in the 8–12 μm region of the electromagnetic spectrum. This prototype instrument was developed for field studies in the earth sciences. THIRSPEC is battery powered, tripod mounted, transportable by backpack, and was designed to collect in situ measurements of ambient spectral thermal emission of targets without disturbing their natural setting [1], [2]. The field of view of THIRSPEC is circular and approximately 12° at full angle. A noise equivalent temperature difference of 0.06°K is obtained using a measurement of 16 standard sets each consisting of 10 1-s readings.

THIRSPEC provides *ground truth* data at the spatial resolution necessary to construct radiative transfer models for the interpretation of airborne and satellite remote sensing data. This study describes the instrument design, summarizes the calibration results for THIRSPEC, and develops a methodology to determine the spectral emissivity of rock samples using this instrument. To minimize angular effects, experiments were conducted under normal viewing geometry.

Manuscript received September 1, 1992; revised September 28, 1993. This work was supported by the Ontario Ministry of Industry, Trade, and Technology, as part of the Ontario Centres of Excellence Program.

B. Rivard, P. J. Thomas, D. Pollex, A. Hollinger, and J. R. Miller are with the Earth Observations Laboratory, Institute for Space and Terrestrial Science, York University, North York, Ont., Canada M3J 3K1.

R. Dick is with Barringer Research Inc., Rexdale, Canada.

IEEE Log Number 9215443.

TABLE I
INSTRUMENT SPECIFICATIONS

Size: Optical head is 43 × 23 × 15 cm
Weight: 30 kg including battery pack, data logger, optical head, cables, and tripod
Battery pack: 5 kg weight, 2–3 h of operation
Slit dimension: 0.2 × 3.0 mm
Grating: 50 LP/mm blazed at 9 μm
Lens: germanium triplet 25 mm EFL, f/0.8
Detector array: DT-591A/UA 60 element HgCdTe Military Common Module
Cryocooler: CTI Cryogenics Model CM-5 closed-Stirling cycle cooler. Working fluid is helium. Cooling capacity 0.35 W/80 K
Spectral resolution: Nyquist limited 0.16 μm
Noise equivalent temperature difference: <0.1 K

II. Spectrometer Design

THIRSPEC consists of four units—an optical head, a data logger, a pack frame, and a tripod. The specifications of the instrument are summarized in Table I. The optical head contains a chopper, reference black body, grating, collimation and focusing optics, detector, detector cooler, amplifiers, and multiplexers. The data logger has a membrane keypad, a 4-line-by-16-character display, five multiplexed 12-bit A/D converter inputs, digital output channels for control of the optical head, three pulse counters, and a serial communication link (RS232). The pack frame contains the battery pack and has attachment features for the optical head, data logger, and tripod. Two cables provide power from the battery pack to the optical head and serial communication between the head and the data logger. In use, the head is usually mounted on the tripod, with the long axis approximately horizontal. An integral beam-steering mirror is pivoted about this axis to view any target between nadir and zenith.

The optical head and data logger are shown schematically in Fig. 1. Thermal radiation entering the head through the entrance slit is reflected off the gold-coated beam-steering mirror, passed through a slit aperture, reflected off a parabolic mirror which collimates the light and illuminates the plane blazed reflection grating. The parallel beam is then focused through a germanium triplet lens that images the slit onto the detector array, a 60-element HgCdTe Common Module detector with integral cryocooler. THIRSPEC compares the exitance of the target to that of an internal black body source at ambient

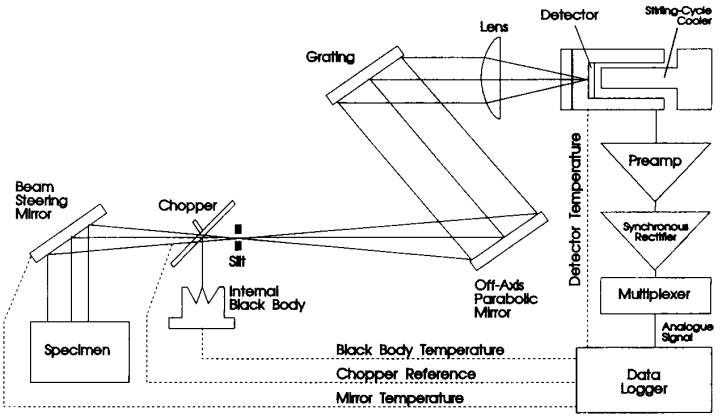

Fig. 1. Schematic diagram of the sensor head of THIRSPEC.

temperature by means of a chopper. Synchronous rectification is performed to eliminate electrical biases and signals from outside the instrument field of view. The voltage difference for each detector element is amplified, synchronously rectified, and multiplexed onto an analog output line. Four output lines handle the 60 voltage readings together with temperature readings for the reference black body, the detector array, and the THIRSPEC enclosure. Finally, the analog signals are passed to the data logger for digitization (12 b), display, and storage. Alternately, the optical head can interface with a microprocessor via a parallel port and a data conversion board.

A. Optics

The first element of the optics is a flat beam-steering mirror which is used to redirect the field of view. A shroud and integral mounting of the steering mirror on the instrument body ensure that the temperature of the steering mirror is always near that of the internal temperature of the instrument. The mirror has a gold coating of low emissivity (about 0.035), and hence there is little self-emission from the steering mirror surface that faces the field of view of the instrument. The temperature of the beam-steering mirror is monitored. An entrance slit and an off-axis parabolic mirror produce a parallel beam to illuminate the grating. The grating aperture (circular) defines the field stop, and the spectrum is imaged onto the detector array by a lens. The path of the principal ray at the blaze wavelength is folded, in the form of a letter "N," in a plane parallel to the base of the spectrometer, and the orientation of the grating rulings is such that the plane of dispersion is almost perpendicular to the base. Fig. 1 shows the plane of the base; the detector is oriented with its long axis perpendicular to this plane. The entrance slit has dimensions of 0.2 × 3.0 mm and is laser-machined in 0.013-mm-thick stainless steel. The entrance slit is imaged with 3.7 demagnification (0.8 mm at the array) onto the detector array.

Since it is hoped to commercialize the THIRSPEC, only stock components are used. All reflecting surfaces are vacuum gold coated. A diamond-turned gold-coated off-axis parabolic mirror is used as the collimator optic because, with the entrance slit at the focus, it is free of spherical and chromatic aberration. The parabola is a 50-mm-diameter 125-mm EFL, with the principal ray at an angle of 30° to the axis. These dimensions, combined with the 25 mm diameter of the aperture at the grating, give the system an external field of view of 0.2 rad (11.4°) and allow a compact optical layout.

The line spacing and blaze for the grating, and the focal length of the lens, are such that the wavelength range of the detector common module just fills the length of the array. Because the closest grating stock values did not produce an exact fit, the dispersion was adjusted by rotating the grating rulings out of the plane of incidence, and adjusting the angle of incidence. Such an "out-of-plane" arrangement results in a large angle between the incident and diffracted beams at the blaze, and permits a more compact optical layout.

The lens is a 25-mm EFL, f/0.8, germanium triplet, diffraction limited over the ±6.7° angle subtended by the array, giving an effective blur of about 12 μm, less than 25% of the detector element dimension of 58 μm in the dispersion direction. The grating aperture rather than the lens aperture was designed to be the limiting aperture of the system. System misalignment can cause wavelength-dependent changes in the field of view.

THIRSPEC operates with modulated radiation and narrow-band ac electronics. The modulator, a chopper disc with twelve uniformly spaced circular openings, is positioned just outside the entrance slit. Consequently, the spectrometer alternately sees the internal reference black body, by reflection off the chopper, and the target, by reflection off the external beam-steering mirror. If the mirror and chopper have identical emissivities and temperatures, the modulated signal depends only on the radiance difference between the target and reference. Because both elements are vacuum coated with gold, in the same lot, the emissivity differences and the resultant radiance errors are small. The chopping frequency is 1 kHz. An optical

pickup on the chopper disc provides a tachometer waveform for the motor drive, and a phase reference for the synchronous rectifiers. The relative sizes of the chopper holes and the input beam (in the plane of the chopper) give a trapezoidal signal waveform, with transition regions (when the edge of a hole is passing through the beam) lasting 14% of a period. The detector signals during transitions are ignored, giving a duty cycle of 0.72.

B. Internal Reference Black Body

The internal reference is an isothermal, ambient-temperature black body cavity of the cylindro-inner-cone form described and analyzed by Bedford *et al.* [3]. When painted, cavities of this shape have both high (>0.99) and uniform effective emissivities along the cone and adjacent cylindrical surface, allowing a short cavity length. The temperature of the cavity is measured but is not actively controlled, which has the advantage of reducing weight, size, power, dynamic range, as well as the accuracy with which the system responsivity must be determined. The reference cavity is small, enclosed in the optical head, and is allowed to stabilize with the ambient environment prior to acquisition. For these reasons, effects of temperature variations within the cavity were found to be negligible during a 1-s measurement.

The radiometric accuracy is dependent on the accuracy of the temperature of the internal reference black body. THIRSPEC uses Platinum Resistance Thermometers (PRT's) to provide an overall temperature accuracy of better than ± 0.1 K. These devices are nominally 100 Ω and 4000 ppm/degree K at 273 K and are individually calibrated to ± 0.0025 K. The bridge circuitry is thermally compensated and designed to have an absolute accuracy of ± 0.02 K at 273 K, and $+0.05$ K from 263 to 308 K. The bridge output is normalized so that the range 263–308 K just fills the 12-b range of the data logger, giving a digitizer resolution of 0.01 K.

C. Detector and Cryocooler

The detector is a 60-element HgCdTe array/dewar package. Each detector element has an area of 58 μm $\times$ 41 μm and is separated from neighboring detectors by 43 μm. The common module array holding the 60 detectors is 6.02 mm in length. This is a mature technology, providing the multiplex advantages of an array at much lower cost than a custom package. Also, compatible lightweight closed-cycle coolers are available. The nominal spectral band of the array is 7.7 ± 0.25 to 11.75 ± 0.25 μm. The temperature of the array is measured with a transistor sensor attached to the focal plane.

The detector array employs a Stirling-cycle cooler designed to be used with military FLIR systems. The cooling capacity is 0.35 W at 80 K, and the unit can draw approximately 30 W at 17 VDC. Use of a closed-cycle system eliminates the logistical requirements imposed by compressed gas and provides a weight reduction of approximately 5 kg relative to a Joule–Thompson cooler with a 5-h gas supply (albeit with some reduction of battery life).

D. Electronics and Signal Processing

1) Analog Electronics: The output from each of the 60 detector channels is amplified with a high-gain preamplifier followed by a switchable-gain amplifier, a synchronous rectifier, and a low-pass filter. The nominal noise figure for the preamplifier is 2.5 nV $Hz^{-1/2}$ at 1 kHz. The gain and bandwidth of each channel is set by selection of the gain resistors and with precision trimming potentiometers. All 60 switchable amplifiers are controlled by two common digital lines from the data logger. While the preamplifier stage is broadband, the synchronous rectifier operates at a nominal frequency of 1 kHz as determined by the speed of the mechanical chopper. The system is relatively insensitive to drift in the chopping frequency. The output of the synchronous rectifier passes through a low-pass filter with a bandwidth of 1 Hz. This filter bandwidth dictates the time between instrument readings which has been set at 1 s. The analog outputs of the 60 detector channels, along with temperature signals from the detector, the beam steering mirror, and the reference black body, are multiplexed onto four analog lines that are accessible to external devices at a chassis-mounted connector.

2) Data Logger: The data logger, Omnidata Polycorder Model PC-706, provides six digital control lines to the optical head, to set the gain of the switchable amplifiers and to switch the analog multiplexers. It digitizes, stores, and transmits the signal voltages from each channel of THIRSPEC. The digitizer has 12-b resolution and 0.15% long-term accuracy. The digitization rate is sufficient to allow one complete reading of 63 signals in the 1-s measurement period that is dictated by the time constant of the analog electronics. There is sufficient memory for up to 900 readings to be stored before transmission via an RS232 serial link to an external computer for further analysis. Up to 150 successive 1-s readings of the detector array can be digitally coadded within the data logger to enhance the signal to noise of the output. The data logger also allows a limited amount of manipulation and display of the digital information at a level that is useful during field data acquisition sessions to verify data and procedures. The data logger is powered by a built-in rechargeable, nickel–cadmium battery, which allows a minimum of 5 h of operation. The memory is powered by a long-life lithium battery which maintains data integrity.

III. System Performance

A. Field-of-View Determination

The field of view (FOV) was measured by moving a small heated object (a resistor with long dimension about 1 cm) across the field of view and measuring the THIRSPEC output reading at each position. For these measurements, the distance from the resistor to the entrance slit of THIRSPEC was 33 cm, and the expected geometrical

field of view was a circle of diameter approximately 7.0 cm. Measurements gave a field of view of 12 degrees ± 15% independent of wavelength or orientation.

B. Spectral Calibration

The optical design of THIRSPEC matches the spatial extent of the 60-element detector array to the desired spectral range. The relation between detector number and wavelength was determined by looking at a black body target through a thin absorbing film polystyrene. The transmittance spectrum obtained for this measurement is shown in Fig. 2. This spectrum displays five well characterized infrared absorption features of polystyrene. As can be seen in Fig. 3, the known wavelengths of the five absorptions define a straight line when plotted against the detector number for the observed absorptions. Additional calibration points were obtained using a tunable CO_2 laser (Table 2) with a monochromator to monitor laser line position and stability. Detectors 1 and 60 lie at 7.42 and 12.08 μm, respectively, and the spectral sampling interval is 0.08 μm/element. The maximum deviation of a calibration point from the best linear fit is approximately 0.1 μm.

C. Spectral Resolution

The spectral resolution of THIRSPEC is limited primarily by the angular size of the discrete detectors on the array. Measurements for CO_2 laser light reflected from a diffuse gold panel were used to check the total system resolution. The laser was tuned to a spectral line at 10.52 μm whose intrinsic line width was less than 0.01 μm. The voltage output from THIRSPEC is shown in Fig. 4. The measured full width at half maximum is 0.09 ± 0.01 μm, which is below the calculated Nyquist frequency of 0.16 μm for the array. This measurement confirms that the detector size and spacing are the limiting factors in resolution rather than the lens or input aperture.

D. Radiometric Calibration

THIRSPEC receives radiation from emission targets within its field of view and from sources whose radiation is reflected from these targets. The transfer function of THIRSPEC relates the voltage signal to radiant power striking the detector when the instrument looks at the external target. The signal voltage for any spectral channel, denoted by $S(\lambda)$, can be related to the input power using the following expression:

$$S(\lambda) - S_o(\lambda) = R(\lambda, T_{\text{det}})G(T_{\text{amb}})\left[-P_{bb}(\lambda, T_{bb}) + \sum_{j=1}^{n}\{P_{Ej}(\lambda, T_{\text{samp}j}) + R_{\text{samp}j}P_{\text{Env}j}\}\right] \quad (1)$$

where

$$P_{\text{Env}j} = \sum_{k=1}^{m} P_{\text{Rkj}}(\lambda, T_{\text{Env}j}) \quad (2)$$

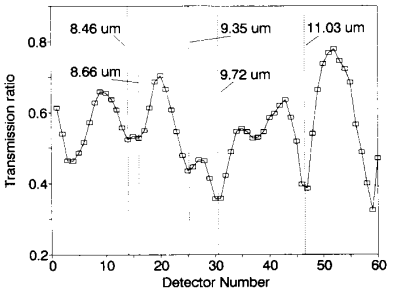

Fig. 2. Transmittance spectrum of polystyrene measured using THIRSPEC. Wavelengths of the labeled absorptions are from Plyer and Peters [4].

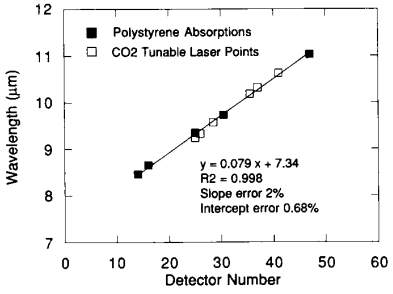

Fig. 3. Spectral calibration of THIRSPEC. Experimental results for absorption wavelengths of polystyrene and reflection wavelengths of CO_2 laser lines.

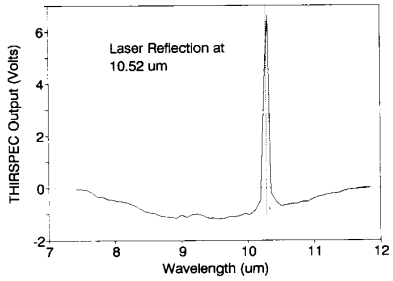

Fig. 4. THIRSPEC signal for CO_2 laser light at 10.52 μm.

TABLE II
TUNABLE CO_2 LASER WAVELENGTHS USED FOR THE SPECTRAL CALIBRATION

Detector	Wavelength (μm)
25	9.24
26	9.33
28.5	9.57
35.5	10.18
37	10.32
41	10.63

and $S(\lambda)$ is the measured voltage, $S_o(\lambda)$ is the offset, $R(\lambda, T_{\text{det}})$ is the responsivity in V W^{-1} of the detector element. Inhomogeneities in the sample and in the environment are handled by the summations in (1). The measured temper-

ature of the entire detector array is T_{det}. The gain of the amplification stages is $G(T_{amb})$ at enclosure temperature T_{amb}. The optical powers, P_{Ej}, P_{Rkj}, and P_{bb}, come from emission sources (within the field of view), reflection sources (outside the field of view), and the internal black body, respectively. R_{sampj} is the reflectivity of the jth region of the sample while T_{bb}, T_{sampj}, and T_{Envk} are the temperatures of the internal black body and the external sources. The optical power, $P_{Ej}(\lambda, T_{sampj})$ at detector λ from emission source j, is assumed to be a black body

$$P_{Ej}(\lambda, T_{sampj}) = \tau_{atm}(\lambda)\tau_{opt}(\lambda)\tau_{grat}(\lambda)\epsilon_j(\lambda)A_j \cdot \frac{\Omega_j}{\pi}\Delta\lambda M(\lambda, T_{sampj}) \quad (3)$$

where τ_{atm}, τ_{opt}, and τ_{grat} are the transmission of the atmospheric path, the optical elements, and the THIRSPEC grating, respectively. In the spectral range covered by THIRSPEC, atmospheric emission in the path between the instrument and the sample is small. The emissivity of source region j is $\epsilon_j(\lambda)$, the effective area of the local homogeneous source region is A_j, the optical bandwidth per wavelength channel is $\Delta\lambda$. The collection solid angle is

$$\Omega_j = \frac{A_{slit}}{D^2}\cos\theta_j \quad (4)$$

where A_{slit} is the area of the entrance aperture of THIRSPEC, D is the distance from the THIRSPEC aperture to the sample, and θ_j is the angle between the aperture normal and the line between the aperture and the sample region A_j. $M(\lambda, T_j)$ is the radiant exitance of the source in units of W cm^{-2} μm^{-1}. A similar expression can be developed for each reflection source and for the internal black body source.

For purposes of radiometric calibration, we used as a sample a well-characterized "black body panel" of known emissivity (close to unity), measured at two temperatures. Temperature of the panel is monitored by a platinum resistance thermometer (PRT) and is actively controlled. The use of a high emissivity target, filling the field of view of THIRSPEC, minimizes the effect of variations of any reflection sources during the measurements. The environment reflection term was constant over the time of the experiment (typically less than 5 min). This assumption was verified by repeating the calibration and by use of a "snout" to change the environment. Changing the temperature of the black body panel, while keeping other parameters constant, allows cancellation of emission from the internal reference black body and reflections from external sources. For two panel temperatures, T_b and T_a, the signal difference is

$$S_b(\lambda) - S_a(\lambda) = K'(\lambda, T_{det}, T_{amb})\epsilon_{samp}(\lambda)A_{samp} \cdot [M(\lambda, T_b) - M(\lambda, T_a)]. \quad (5)$$

The area A_{samp} of the black body panel is the full area of the field of view of the instrument. The radiation equilibrium condition, $R_{samp} = 1 - \epsilon_{samp}$, has been assumed, and

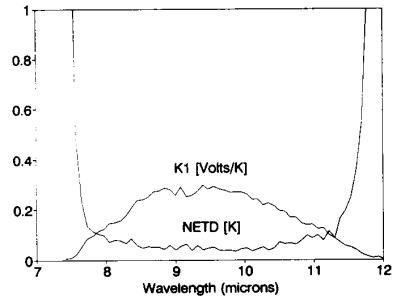

Fig. 5. Radiometric calibration of THIRSPEC. K_1 is the instrument transfer function in volts per degree Kelvin [equation (7)]. NETD is the noise equivalent temperature difference in degree Kelvin. Both are read from the same Y-axis.

$$K'(\lambda) = R(\lambda, T_{det})G(T_{amb})\tau_{atm}(\lambda)\tau_{opt}(\lambda)\tau_{grat}(\lambda) \cdot \frac{A_{slit}}{\pi D^2}\cos\theta_j\,\Delta\lambda \quad (6)$$

in units of V μm W^{-1}. For small temperature differences, (5) becomes

$$S_b(\lambda) - S_a(\lambda) = K'(\lambda, T_{det}, T_{amb})\epsilon_{samp}(\lambda)A_{samp} \cdot \frac{\partial M(\lambda, T_a)}{\partial T}(T_b - T_a) = K_1(T_b - T_a)\epsilon_{samp}(\lambda). \quad (7)$$

The K_1 term for each detector (Fig. 5) in V/K was determined using a least squares fit of small temperature changes $(T_b - T_a)$ for the black body panel near 28°C. T_{amb} is measured with a PRT positioned on the beam-steering mirror. Drift in T_{bb}, T_{det}, and T_{amb} were compensated for in the analysis. Wavelength variations in K_1 are largely caused by the transmission of the optical elements. Although some change in K_1 can be expected at different operating temperatures, this is expected to be relatively small over the temperature range of interest (about 28 ± 5°C).

E. Noise Equivalent Temperature Difference

The noise equivalent temperature difference (NETD) was determined by 16 repetitions of a standard measurement set. Each standard set was the sum of 10 1-s readings of the voltage signal from an external reference black body. The "NETD per channel," plotted on Fig. 5, is the standard deviation of these 16 standard measurements expressed in temperature units through (7). An average NETD of 0.06°K was measured between 7.9 and 11.3 μm with the detector array operating at 119°K. The noise can be reduced by a longer integration time or a cooler detector array.

IV. Retrieval of Target Emissivity

The primary objective of the data analysis is the retrieval of spectral emissivity for unknown geological targets in their natural setting. Because the reflection sources are usually not known and mask the desired emission signal, $P_{\mathrm{Env}j}$ of (1) must be dealt with. A diffuse gold reference is commonly used to determine $P_{\mathrm{Env}j}$ [5], [6]. However, two (or more) previously characterized samples can replace the diffuse gold reference provided there is "sufficient" reflected signal. To use the signals for two samples, (1) is rearranged to explicitly show sample emissivity. For this purpose, we use Kirchoff's law, and the sample is assumed to be a gray body. When T_{bb}, ϵ_{bb}, and $S_o(\lambda)$ [in (1)] are constant for two homogeneous samples, a and b, and T_a and T_b are equal, the signal difference is

$$\frac{S_b - S_a}{K' * A_{\mathrm{samp}} * M_{\mathrm{samp}}} = (\epsilon_b - \epsilon_a)\left(1 - \frac{P_{\mathrm{Env}}}{M_{\mathrm{samp}}}\right) \quad (8)$$

or

$$\left[1 - \frac{P_{\mathrm{Env}}}{M_{\mathrm{samp}}}\right] = \frac{(S_b - S_a)}{(\epsilon_b - \epsilon_a)} \frac{1}{(K' * A_{\mathrm{samp}} * M_{\mathrm{samp}})}. \quad (9)$$

The effect of the emissivity difference term is to magnify the measurement noise in $(S_b - S_a)$ and reduce the accuracy of the determination of the environment factor on the left of (9). When $(S_b - S_a)$ is small (and hence also the environmental factor), the usefulness of the environment correction procedure is sensitive to the NETD of the measurements.

A quartzite and a limestone sample were used to determine P_{Env}, while the "unknown" was a hornblende gabbro. Quartz (silicon dioxide) is the main mineral constituent of the quartzite; limestone consists mostly of calcite (calcium carbonate). These common rock-forming minerals, and the minerals plagioclase and hornblende present in the "unknown," have well-documented fundamental stretching and bending vibrations of Si–O and C–O bonds in the 7–12 μm spectral region [7], [8]. The "known" emissivity spectra were computed from directional hemispherical reflectance measurements as described by Rivard *et al.* [9]. Directional reflectance spectra were acquired at a 10° incidence angle using an Analect Fourier Transform Infrared (FTIR) spectrometer equipped with an integrating sphere attachment. The light source was a heated nichrome wire. Spectral resolution within the 7–12 μm spectrum is 4 cm^{-1} for the FTIR spectra. Each analysis represents the average of 765 scans of the reflected beam from the sample divided by the average of 765 scans from a diffuse gold-coated standard. For natural surfaces which are optically thick, the emissivity in the thermal infrared can be derived from the reflectance using Kirchhoff's law [7], [10]–[13].

The THIRSPEC measurements [S in (8)] on all three samples were performed outdoors in a clearing away from buildings, under clear sky conditions, and in the absence of wind. The instrument was allowed to stabilize for 30 min prior to acquisition. The signals for the samples were obtained from an average of 10 consecutive 1-s readings. PRT's in contact with the rock surfaces and with the air were used to measure T_{samp} and T_{Env}. T_{samp} is used to compute M_{samp} in (8). Typical parameters values measured during the experiment are listed in Table III.

TABLE III
Parameters Used to Model the Reflection Contribution by the Environment

Typical Values Measured	Typical Values Estimated
$T_{\mathrm{det}} = 115°\mathrm{K}$, $T_{\mathrm{amb}} = 282.2°\mathrm{K}$, $T_{bb} = 282.2°\mathrm{K}$,	$T_{\mathrm{env}} = 279.5°\mathrm{K}$
$T_{\mathrm{samp}a} = 280.5°\mathrm{K}$, $T_{\mathrm{samp}b} = 280.5°\mathrm{K}$	$\epsilon_{\mathrm{env}}(\lambda) = 0.6$

In a first step, we used (8), the THIRSPEC signals for quartz and limestone, the parameters listed in Table III, and the known emissivities for the limestone and quartzite samples to compute the term P_{Env}. P_{Env} behaved as a gray body with emissivity of 0.6 and T_{Env} of 279.5 K. Fig. 6 compares the emissivity calculated for the quartzite sample with and without an environmental correction. For reference, the "known" emissivity is shown. Because the environment acts as a gray body, the spectral shape of the environment correction term (Fig. 6) is dominated by the reflectivity of the quartzite sample.

In a second step, equation (8) was used to compute the emissivity of the unknown target which was measured under the same environmental conditions as the limestone and quartzite samples. For this purpose, we used the THIRSPEC signal, the known emissivity of the quartzite, and the values for P_{Env} determined in the first step. Results are shown in Fig. 7. Whereas the uncorrected difference signal shows a blend of emission and reflection that masks the emissivity profile of the unknown, the corrected spectrum shows well-defined mineral emissivity features. Between 8 and 9.4 μm approximately, the uncorrected spectrum shows lower emissivity than the corrected spectrum; the situation is reversed at longer wavelengths. The effect is expected from equation (8) in the scenario where a geological sample (rather than a gold mirror, for instance) is used for the difference spectrum and the radiant exitance of the environment is smaller than that of the sample, either because of a lower temperature or a smaller emissivity. When the emissivity of hornblende is greater than that of quartz, the correction factor in Fig. 7 is positive and the corrected emissivity is larger than the uncorrected one. Similarly, when the emissivity of quartz is larger than that of hornblende, the correction factor is negative and the corrected emissivity is lower than the uncorrected one. A similar effect can be seen on Fig. 6, where the reference sample is limestone. Over most of the spectrum, limestone has a larger emissivity than quartz and the corrected emissivity is less than the uncorrected one. Near 11.3 μm, the limestone emissivity dips to 0.83 and the situation is reversed. This effect is reduced by the increased instrument noise at the edges of the spectral passband. Between 7.9 and 11.3 μm, where the responsivity of THIRSPEC is high and the NETD is

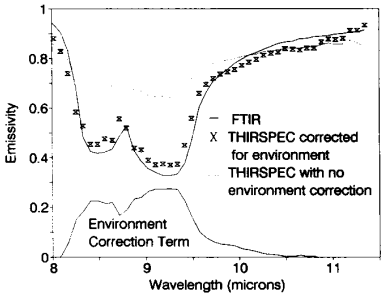

Fig. 6. Fitting the THIRSPEC quartz emissivity spectrum to the FTIR reference spectrum, to obtain the environmental emission reflecting off the target. The dotted curve represents the quartzite spectrum if environmental reflections are neglected. The solid curve, labeled "environment correction term," was obtained from the difference of the reflection-corrected (X symbol) and uncorrected curves (dotted curve) [P_{Env}/M_{samp} in equation (8)], illustrating the modulation of the environment by the target sample. Parameters used in the fit are listed in Table III.

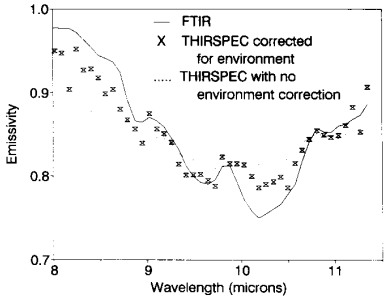

Fig. 7. Comparing the hornblende gabbro emissivity spectra, corrected (X symbol) and uncorrected (dotted curve) for reflections from the environment, with the FTIR reference emissivity spectra for the hornblende gabbro (solid curve). ϵ_{envk} and T_{envk} were determined using the quartzite and limestone spectra as described in Section IV.

low, the corrected emissivity of the unknown is comparable to that obtained under well-controlled conditions using FTIR spectroscopy. Residual differences between the known (FTIR) spectrum and the THIRSPEC corrected spectrum are consistent with the spatial variability of the emissivity over the hornblende gabbro sample. At present, the effect of sample temperature variations and similar error sources have not been assessed.

V. Summary and Conclusions

The THIRSPEC instrument has a usable spectral range of 7.9–11.3 μm. Over this spectral range, the noise equivalent temperature difference (NETD) is <0.1 K for a measurement of 16 standard sets each consisting of 10 1-s readings. A major limitation on the spectral range comes from the band-limiting filters of the Military Common Module. Use of a similar detector with slightly different filters would allow the range to be extended and the detection of the carbonate absorption near 11.3 μm [8]. The resolution is at the Nyquist frequency limit of 0.16 μm as determined by the size and spacing of the detector elements.

THIRSPEC is a portable thermal infrared spectrometer which can be transported and operated in the field by two people. Calibration in the field is not required. As part of this study, measurements of spectral emissivity have been obtained from rock samples both in the laboratory and under field conditions. The use of reference geological samples allows the effect of reflected background radiation from the instrument and from the environment to be removed under most conditions.

Acknowledgment

THIRSPEC was fabricated by Barringer Ltd. and evaluated by the Institute for Space and Terrestrial Science, Toronto, Canada. We are grateful to J. Crisp for her assistance during acquisition of FTIR reflectance spectra at the Jet Propulsion Laboratory.

References

[1] F. Nerry, J. Labed, and M. P. Stoll, "Emissivity signatures in the thermal IR band for remote sensing: Calibration procedure and method of measurement," *Appl. Opt.*, vol. 27, pp. 758–764, 1988.

[2] Y. W. Zhang, C. G. Zhang, and V. Klemas, "Quantitative measurements of ambient radiation, emissivity, and truth temperature of a greybody: Methods and experimental results," *Appl. Opt.*, vol. 25, p. 3683, 1986.

[3] R. E. Bedford, C. K. Ma, Y. Chu, and S. Chen, "Emissivities of diffuse cavities. 4: Isothermal and nonisothermal cylindro-inner-cones," *Appl. Opt.*, vol. 24, pp. 2971–2980, 1985.

[4] E. K. Plyer and C. W. Peters, "Wavelengths for calibration of prism spectrometers," *J. Res. Nat. Bureau Standards*, vol. 45, pp. 462–466, 1950.

[5] J. W. Salisbury, "First use of a new portable thermal infrared spectrometer," in *Proc. IEEE Int. Geosci. Remote Sensing Symp.*, vol. 3, 1990, pp. 1775–1778.

[6] J. W. Salisbury and D. M. D'Aria, "Emissivity of terrestrial materials in the 8–14 μm atmospheric window," *Remote Sensing Envir.*, vol. 42, pp. 83–106, 1992.

[7] J. W. Salisbury and L. S. Walter, "Thermal infrared (2.4–13.5 μm) spectroscopic remote sensing of igneous rock types on particulate planetary surfaces," *J. Geophys. Res.*, vol. 94, pp. 9192–9202, 1989.

[8] J. W. Salisbury, L. S. Walter, N. Vergo, and D. M. D'Aria, *Infrared (2.1–25 μm) Spectra of Minerals*. Baltimore, MD: The John Hopkins University Press, 1992.

[9] B. Rivard, S. Petroy, and J. Miller, "Measured effects of desert varnish on the mid-infrared spectra of weathered rocks as an aid to TIMS imagery interpretation," *IEEE Trans. Geosci. Remote Sensing*, vol. 31, pp. 284–291, 1993.

[10] F. E. Nicodemus, "Directional reflectance and emissivity of an opaque surface," *Appl. Opt.*, vol. 4, pp. 767–773, 1965.

[11] E. Schanda, *Physical Fundamentals of Remote Sensing*. Berlin: Springer-Verlag, 1986.

[12] A. B. Kahle, M. S. Shumate, and D. B. Nash, "Active airborne infrared laser system for identification of surface rock and minerals," *Geophys. Res. Lett.*, vol. 11, pp. 1149–1152, 1984.

[13] M. J. Bartholomew, A. B. Kahle, and G. Hoover, "Infrared spectroscopy (2.3–20 μm) for the geological interpretation of remotely-sensed multispectral thermal infrared data," *Int. J. Remote Sensing*, vol. 10, pp. 529–544, 1989.

Benoit Rivard received the B.Sc. and M.Sc. degrees in geology from McGill University, Montreal, P.Q., Canada, in 1983 and 1985, respectively; and the Ph.D. degree in earth and planetary sciences from Washington University, St. Louis, MO in 1980.

He is currently a Project Scientist at the Earth Observations Laboratory of the Institute for Space and Terrestrial Science, Toronto. His research includes the use of ground and airborne multispectral remote sensing for lithologic and structural

mapping, applications of spectral unmixing techniques for mapping, the infrared characterization of terrestrial materials, and the development of methodologies for precise field measurement of emissivity.

Paul J. Thomas received the B.Sc., M.S., and Ph.D. (1977) degrees in physics from the University of Toronto.

Since 1990 he has been a Staff Scientist at the Institute for Space and Terrestrial Science, North York, Ont., where his research interests are in the application of infrared sensor technology.

D. Pollex, photograph and biography not available at time of publication.

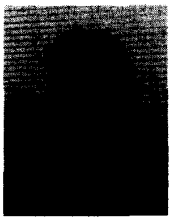

A. Hollinger has been engaged in optical research and in electro-optical system design. His research has focused on the design, evaluation, and deployment of airborne and ground-based spectroscopic instrumentation for use in remote sensing of the earth's surface. At the time this work was conducted, he was the Manager of the Electro-Optics Laboratory at the Institute for Space and Terrestrial Science.

Dr. Hollinger is a member of OSA, SPIE, and CAP.

John R. Miller received the B.E. degree in physics from the University of Saskatchewan, Sask., in 1963, and the M.Sc. and the Ph.D. degrees in space physics from the same university, in 1966 and 1969, respectively, studying the aurora borealis using rocket-borne radiometers.

He then spent 2 years on a Postdoctoral Fellowship at the Herzberg Institute at the National Research Council in Ottawa. In 1971 he went to work as a Project Scientist at York University and obtained a faculty appointment in 1972. He is currently Professor of Physics and Astronomy at York University, and is Co-Director of the Earth Observations Laboratory of the Institute for Space and Terrestrial Science. His remote sensing research interests have included interpretation of water color reflectance, atmospheric correction, and canopy reflectance. Over the past 6 years his primary focus has been on the application of reflectance spectroscopic techniques in remote sensing using imaging spectrometers.

R. Dick, photograph and biography not available at time of publication.